Evidence of neocortex-like primitive laminar pallium in avian embryo & its organization by microRNA-19b

Suvimal Kumar Sindhu[1], Archita Mishra, Niveda Udaykumar[2], Jonaki Sen*

Indian Institute of Technology Kanpur, Kanpur-208016, UP, India

[1]Yale School of Medicine, New Haven, CT, 06511, USA

[2] St. Jude Children's Hospital, Memphis, TN, 38105, USA

***Email:** jonaki.sen@iitk.ac.in

Author Contributions:

S.K.S., and J.S. designed research; S.K.S., A.M., N.U. performed research; S.K.S., A.M., N.U., and J.S. analyzed data; J.S. Supervised; S.K.S., A.M., and J.S. wrote the paper.

Competing Interest Statement: No competing interest.

Classification: Major: Biological Sciences; **Minor:** Neuroscience

Keywords: miR-19b, Fezf2, Pallium, Chick, Mef2c, Neocortex

This file includes:

Main Text
Figures 1 to 2

Abstract

The avian pallium contains spatially segregated clusters of neurons, unlike mammalian neocortex, where neurons are highly organized as a six-layered structure. However, the quest to find similarities between avian pallium and mammalian neocortex has long been pursued. The extent of similarity among embryonic avian pallium and mammalian neocortex in terms of pallial organization is not completely explored. Our expression analysis revealed existence of a transient two-layer lamina in the developing chick pallium, mirroring the order of neocortical layers as well as the proliferation-dependent mode of specification that is partly regulated by microRNA-19b. This suggests a closer ontogenetic similarity between avian pallium and mammalian neocortex, reinforcing the idea of convergent evolution of cortical lamina from common amniote ancestry.

Main Text

Introduction

The evolution of laminar pallium like mammalian neocortex from nonlaminar pallium of birds and reptiles is a long-standing interest in the field of neuroscience (1, 2). The mammalian neocortex features a six-layered laminar pallium, with neocortical neurons following an inside-out birth and migration pattern (3). However, unlike mammals, avian pallial neurons follow an outside-in pattern, with first-born neurons atop and subsequent neurons migrating beneath, and specified as spatially segregated nuclei instead of laminar structures (4). However, birds exhibit region-specific laminar organization in the primary auditory cortex (5), the hyperpallium region (6). Moreover, examination of expression of homologous neocortical layer markers and, projections of developing avian pallial nuclei reveals presence of neocortex-like neuronal subtypes (1, 7, 8). Nevertheless, initial steps and mechanisms of formation of such homologous neurons in avian brain are not well studied. Hence, in this study, we compared expression pattern of deep-layer neocortical marker (Fezf2) and upper-layer marker (Mef2c) (2) in early stages of avian pallial development and explored its similarity with neocortical organization as well as mode of production.

Results & Discussion

To comprehensively analyze expression pattern of Fezf2 & Mef2c markers in the avian system, we used embryonic day (E) 5.5, or Hamilton-Hamburger stage (HH) 28 (9) and E7.5 (HH32) and found that at E5.5, Fezf2 was found to be expressed in the ventricular zone (VZ) of the dorsomedial region and the subventricular zone (SVZ) of dorsal pallium (Fig. 1A). To further ascertain the identity of these Fezf2+ SVZ cells, we performed immunostaining of Neurod1, a postmitotic immature neuron marker, on these sections and found out that indeed these Fezf2+cells were co-expressing Neurod1 (Fig.1A, Inset), suggesting that these Fezf2+ cells in the SVZ are postmitotic immature neurons. Furthermore, Mef2c expression was found atop Fezf2+ neurons of the SVZ (Fig. 1A). Hence, Fezf2 and Mef2c present a bi-layer structure at E5.5, mirroring the order of neocortical lamina (2).

However, at advanced stages i.e. E7.5 (Fig. 1B), E10 and post-natal day (P) 0, expression domain of these two markers get spatially segregated, Fezf2 in the hyperpallium and parahippocampal area (APH) and Mef2c in the mesopallium (Msp) (1, 8). Therefore, in the

avian pallium at later stages, both Fezf2+ and Mef2c+ neurons are spatially segregated unlike earlier stage with bi-layered structure. Evidence of such transient lamina at early avian forebrain suggests that the common ancestors of birds and mammals may have at least primitive pallial lamina such as this.

Further, to understand the mechanism of appearance of Fezf2 expression in the deep-layer at E5.5, we took cues from mouse study where deep-layer neurons appear because of early cessation of neurogenesis (10, 11). Hence, to find correlation between proliferation and the induction in the expression of Fezf2 in the deep-layer/SVZ in the chick embryo, we analyzed the dynamics of proliferation in the developing chick pallium. The analysis of proliferation at E4.5 (HH25) using PH3-immunostaining showed homogenous proliferation across the dorsal pallium, however at E6.5 (HH30) proliferation ceases at the dorsomedial region and the lateral region at DVR showed continued proliferation, further at E8.5 (HH35) proliferation was not observed, similar to previous studies (Fig. 1C) (7, 8). Moreover, Neurod1 showed negligible expression at E4.5, however at the E6.5 it was predominant in the SVZ of wulst area subsequently, at E8.5 it showed biased expression at the SVZ of DVR area only, however some expression was found in the Hippocampal and APH region as well (Fig.1C), (7). Taken together, these data show that NPCs at the dorso-medial region cease proliferation earlier than the dorso-lateral region. Hence it is postulated that early inhibition of proliferation of NPCs can produce Fezf2+ neurons.

Interestingly, NPCs in the developing chick embryo show spatially-biased potential in generation of Fezf2+ and Mef2c+ neurons, however in contrast *in vitro* study showed that chicken NPCs can generate both deep-layer and upper-layer neurons, similar to mammals (8, 11). Hence, to test the role of cell-cycle in formation of deep-layer neurons, we electroporated a DNA construct that expresses CDKN1A, a cell-cycle inhibitor (12) in the early chick forebrain this induced ectopic expression of Fezf2+; Neurod1+ neurons (Fig. 1D). This suggests that the cell-cycle perturbation is sufficient to regulate the formation of Fezf2+; Neurod1+ neurons in the developing chicken pallium (Fig. 1D).

Further, to find out a cell-cycle regulator for this context, we used literature search and selected a microRNA, miR-19b that regulates proliferation in the mouse forebrain (13) and express in the chick pallial VZ at E4.5 (14). Our analysis showed miR-19b expression in the proliferating NPCs at VZ at E6.5 as well, as opposed to the Neurod1 in the SVZ (Fig.1E).

Further, to better establish the role of miR-19b in proliferation, we analyzed *in silico* predicted target mRNAs identified by miR database (miRDB) (15) and Targetscan (16), its intersection showed 424 potential targets (1F). Gene ontology analysis showed that several genes regulated by miR-19b are related to cellular senescence (Fig. 1F, G). Moreover, based-on robust expression in the developing chick forebrain, we selected two well-known inhibitors of cell-cycle i.e. E2f8 and Neurod1 (7, 17).

Now, to test the effect of miR-19b on E2f8 and Neurod1 mRNAs, we performed gain-of-function (GoF) and loss-of-function (LoF) experiments with miR-19b using expression construct for miR-19b and Sponge-19b, respectively (See materials and methods) (14), and found out that miR-19b is indeed sufficient to regulate the expression of E2f8 as well as Neurod1, whereas necessary for E2f8 expression but Neurod1 (Fig. 1H-K). Lack of ectopic expression of Neurod1 upon LoF experiment suggest that there could be presence of other inhibitory factors for Neurod1 in these regions of brain.

Further, we analyzed target regions of E2f8 and Neurod1 across different species using TargetScan (16) this showed evolutionary conserved target regions (Fig. 2A, C). Next, we tested if miR-19b can regulate these transcripts through their respective target regions. For this, we performed sensor assay (14), by expressing fused transcripts of target regions of E2f8 and Neurod1 with mCherry reporter coding sequence (CDS) co-expressed with miR-19b and control constructs (Fig. 2B, D). This lead to downregulation of mCherry expression by miR-19b expression in comparison to control indicating miR-19b can regulate these transcripts using their target regions and may have a role in regulation of proliferation.

Further to establish the role of miR-19b in cell-cycle regulation, we used flow cytometer to measure the DNA quantity in chicken fibroblast cells (DF1) transfected with miR-19b and control constructs, this promoted cells in S-phase and M-phase whereas reducing G0/G1 in comparison to control (Fig. 2E, F). To test the ability of miR-19b in regulation of cell cycle in the developing chick pallium, we used EdU, a thymidine analog, that gets incorporated in the DNA during S-phase of the cell-cycle. For this, we expressed miR-19b, Sponge-19b and control constructs in chick embryo forebrain at E3.5 (HH23) and 2 hours before harvesting i.e. E4.5 (HH25), EdU was overlaid. The analysis of EdU+; GFP+ cells over total GFP+ cells revealed that indeed miR-19b can promote incorporation of EdU whereas Sponge-19b can reduce EdU labelling in comparison to control (Fig. 2G). Further, to analyze effect on M-phase, we performed GoF and LoF experiments with miR-19b at E8 and found out indeed miR-19b overexpression promotes GFP+; PH3+ over total GFP+ cells whereas deficiency of miR-19b inhibited that, in comparison to the control (Fig. 2H). Taken together, these data suggests that miR-19b have a role in proliferation in the early chick embryo.

Having established miR-19b as a regulator of cell cycle inhibitor, and our observation of cell cycle inhibition leading to ectopic Fezf2 expression (Fig. 1D), prompted us to test if LoF experiment with miR-19b can promote expression of deep-layer marker, Fezf2. For this, we expressed Sponge-19b in the VZ and showed that indeed removal of miR-19b lead to ectopic expression of Fezf2+ neurons in comparison to the control (Fig. 2H). This type of proliferation based mechanism of specification of pallial neurons is similar to the neocortex neuronal specification (10). Hence this indicates that the mechanism of cell cycle-mediated specification of laminar neurons are present in the primitive species than the mammals.

One of the crucial features of deep-layer neurons in the neocortex is sub-cerebral/extra-telencephalic long-range projections to establish cortico-spinal tract. In mammals, Fezf2 is critical for specification of deep-layer neurons and their emerging projections (18). In the avian system, since laminar Fezf2+ immature neurons are transient in nature and occur at an early stage of pallial development it is impossible to study conservation in projections for these neurons as projections emerges from relatively more mature neurons. However, at later stages of development, Fezf2+ neurons are found to be robustly expressed in the rostral hyperpaliium region of the somatosensory wulst (1) and interestingly, neurons from this region, show similar long-range projection to the red nucleus apart from other nuclei, this further projects to the spinal cord (19), therefore, this supports the idea that Fezf2 has similar potential as that of mammalian brain; (a) in generating long-range projection even though at later stage of development and, (b) presence of Fezf2+ neurons in the deep-layer in the early chick embryo supports the view of correlation between deep-layer and long-range projection albeit at different stages.

Additionally, since dorsal DVR region show prolonged proliferation and Mef2c- an upper layer marker expression observed at the lateral DVR i.e. mesopallium, suggest implication of prolonged proliferation in upper-layer-like neuron formation, similar to the mammalian (8). However, at earlier stages where NPCs are still early in terms of proliferation, only two possible mechanisms that can explain bi-layer structure, a) conversion of Fezf2+ neurons to Mef2c+ neurons by achieving knock-down of Fezf2 expression, this is supported by the fact that Fezf2 LoF lead to conversion for DL neurons into UL neurons in the mouse (18), b) Migration of relatively earlier born NPCs, than the NPCs that generate Fezf2+ neurons passing through Fezf2+ neurons situating atop above those, this is less likely to happen as avian species mainly show outside-in pattern of migration (4).

In conclusion, we have shown that birds do have a primitive laminar organization akin to mammalian neocortex in terms of organization and cell-cycle dependent mode of production of neurons. Hence, this suggests that birds and mammals may have a common ancestry with similar mode of laminar pallial formation.

Materials and Methods

The chicken eggs form white leg horn hen were obtained from Kanpur, India.
Experimental details are provided in Supplementary Information.

Data Availability

All data included in the manuscript.

Acknowledgments

We acknowledge Prof. Amitabha Bandhopadhyay (IIT Kanpur, India) for valuable suggestions on the manuscript. We are grateful to Neetu Dey (IIT Kanpur) for confocal microscopy, and D. N. Vishwakarma (CDRI, Lucknow) for flow cytometry. This work was funded by SERB, Department of Science & Technology, Govt. of India. (EMR/2016/000886) to J.S. CSIR, Govt. of India supported S.K.S. for his Ph.D. (09/092(0824)/2011-EMR-I). A.M. and N.U. were supported by MHRD, Govt. of India.

References

1. J. Dugas-Ford, J. J. Rowell, C. W. Ragsdale, Cell-type homologies and the origins of the neocortex. *Proc Natl Acad Sci U S A* **109**, 16974-16979 (2012).
2. B. J. Molyneaux, P. Arlotta, J. R. Menezes, J. D. Macklis, Neuronal subtype specification in the cerebral cortex. *Nat Rev Neurosci* **8**, 427-437 (2007).
3. J. B. Angevine, Jr., R. L. Sidman, Autoradiographic study of cell migration during histogenesis of cerebral cortex in the mouse. *Nature* **192**, 766-768 (1961).
4. H. M. Tsai, B. B. Garber, L. M. Larramendi, 3H-thymidine autoradiographic analysis of telencephalic histogenesis in the chick embryo: I. Neuronal birthdates of telencephalic compartments in situ. *J Comp Neurol* **198**, 275-292 (1981).
5. Y. Wang, A. Brzozowska-Prechtl, H. J. Karten, Laminar and columnar auditory cortex in avian brain. *Proc Natl Acad Sci U S A* **107**, 12676-12681 (2010).

6. M. Stacho *et al.*, A cortex-like canonical circuit in the avian forebrain. *Science* **369** (2020).
7. S. Gupta, R. Maurya, M. Saxena, J. Sen, Defining structural homology between the mammalian and avian hippocampus through conserved gene expression patterns observed in the chick embryo. *Dev Biol* **366**, 125-141 (2012).
8. I. K. Suzuki, T. Kawasaki, T. Gojobori, T. Hirata, The temporal sequence of the mammalian neocortical neurogenetic program drives mediolateral pattern in the chick pallium. *Dev Cell* **22**, 863-870 (2012).
9. V. Hamburger, H. L. Hamilton, A series of normal stages in the development of the chick embryo. 1951. *Dev Dyn* **195**, 231-272 (1992).
10. S. K. McConnell, C. E. Kaznowski, Cell cycle dependence of laminar determination in developing neocortex. *Science* **254**, 282-285 (1991).
11. Q. Shen *et al.*, The timing of cortical neurogenesis is encoded within lineages of individual progenitor cells. *Nat Neurosci* **9**, 743-751 (2006).
12. C. Deng, P. Zhang, J. W. Harper, S. J. Elledge, P. Leder, Mice lacking p21CIP1/WAF1 undergo normal development, but are defective in G1 checkpoint control. *Cell* **82**, 675-684 (1995).
13. S. Bian *et al.*, MicroRNA cluster miR-17-92 regulates neural stem cell expansion and transition to intermediate progenitors in the developing mouse neocortex. *Cell Rep* **3**, 1398-1406 (2013).
14. S. K. Sindhu, N. Udaykumar, M. A. A. Zaidi, A. Soni, J. Sen, MicroRNA-19b restricts Wnt7b to the hem, which induces aspects of hippocampus development in the avian forebrain. *Development* **146** (2019).
15. Y. Chen, X. Wang, miRDB: an online database for prediction of functional microRNA targets. *Nucleic Acids Res* **48**, D127-D131 (2020).
16. V. Agarwal, G. W. Bell, J. W. Nam, D. P. Bartel, Predicting effective microRNA target sites in mammalian mRNAs. *Elife* **4** (2015).
17. J. Christensen *et al.*, Characterization of E2F8, a novel E2F-like cell-cycle regulated repressor of E2F-activated transcription. *Nucleic Acids Res* **33**, 5458-5470 (2005).
18. B. Chen *et al.*, The Fezf2-Ctip2 genetic pathway regulates the fate choice of subcortical projection neurons in the developing cerebral cortex. *Proc Natl Acad Sci U S A* **105**, 11382-11387 (2008).
19. L. Medina, A. Reiner, Do birds possess homologues of mammalian primary visual, somatosensory and motor cortices? *Trends Neurosci* **23**, 1-12 (2000).

Figures

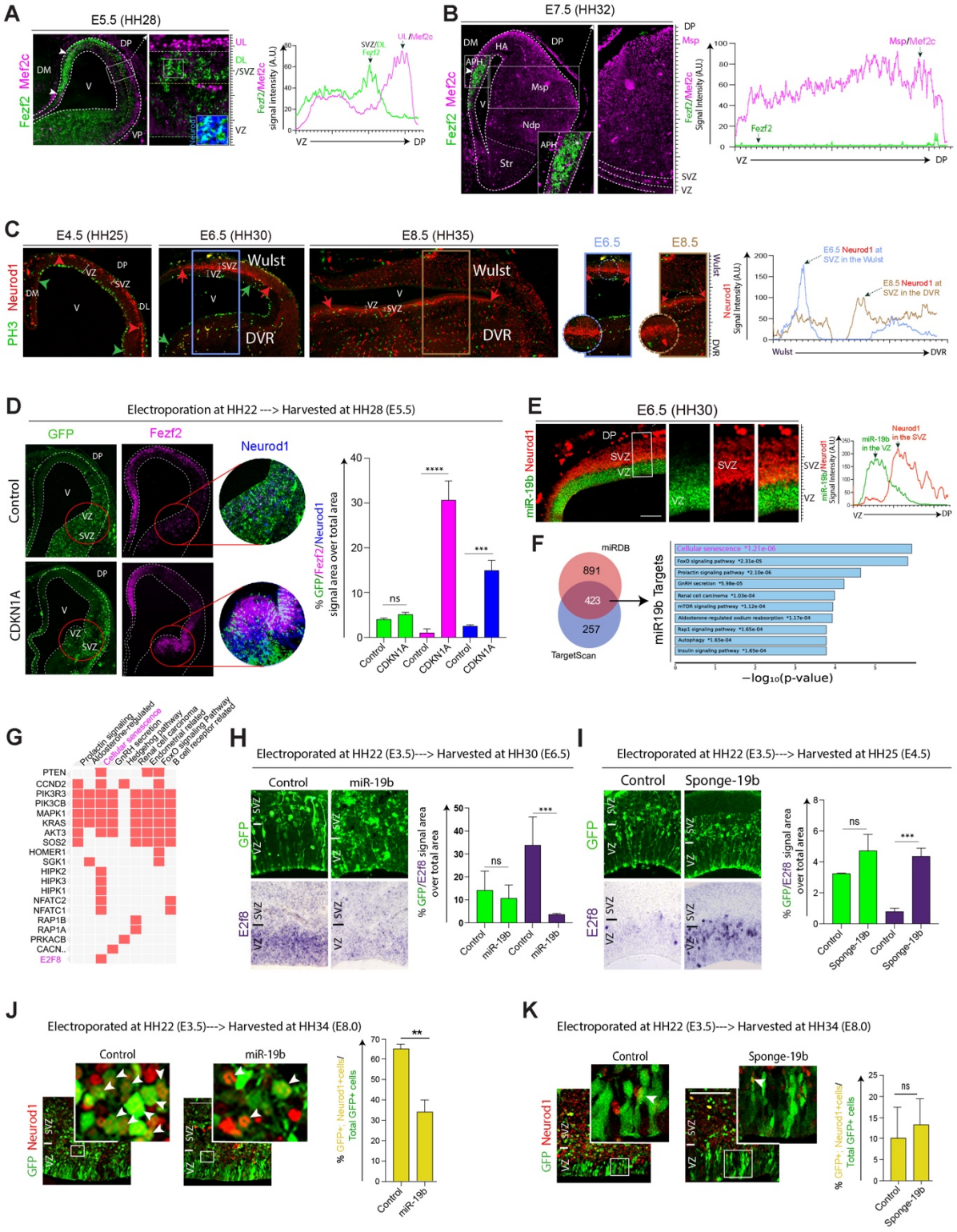
A
E5.5 (HH28)
Fezf2 Mef2c
DM
V
DP
VP
UL
DL
/SVZ
VZ
Fezf2/Mef2c signal intensity (A.U.)
SVZ/DL
Fezf2
UL /Mef2c
VZ
DP
B
E7.5 (HH32)
DM
HA
DP
APH
Msp
Ndp
Str
Fezf2 Mef2c
Msp
Fezf2/Mef2c
Signal Intensity (A.U.)
Msp/Mef2c
Fezf2
SVZ
VZ
C
E4.5 (HH25)
E6.5 (HH30)
E8.5 (HH35)
Neurod1
PH3
Wulst
DVR
E6.5
E8.5
Neurod1
Signal Intensity (A.U.)
E6.5 Neurod1 at SVZ in the Wulst
E8.5 Neurod1 at SVZ in the DVR
Wulst
DVR
D
Electroporation at HH22 ---> Harvested at HH28 (E5.5)
GFP
Fezf2
Neurod1
Control
CDKN1A
% GFP/Fezf2/Neurod1 signal area over total area
****
***
ns
Control
CDKN1A
E
E6.5 (HH30)
miR-19b Neurod1
DP
SVZ
VZ
miR-19b/Neurod1 Signal Intensity (A.U.)
miR-19b in the VZ
Neurod1 in the SVZ
F
miRDB
891
423
257
TargetScan
miR19b Targets
Cellular senescence *1.21e-06
FoxO signaling pathway *2.31e-05
Prolactin signaling pathway *2.10e-06
GnRH secretion *5.98e-05
Renal cell carcinoma *1.03e-04
mTOR signaling pathway *1.12e-04
Aldosterone-regulated sodium reabsorption *1.17e-04
Rap1 signaling pathway *1.65e-04
Autophagy *1.65e-04
Insulin signaling pathway *1.65e-04
−log10(p-value)
G
Prolactin signaling
Aldosterone-regulated
Cellular senescence
GnRH secretion
Hedgehog pathway
Renal cell carcinoma
Endometrial related
FoxO signaling pathway
B cell receptor related
PTEN
CCND2
PIK3R3
PIK3CB
MAPK1
KRAS
AKT3
SOS2
HOMER1
SGK1
HIPK2
HIPK3
HIPK1
NFATC2
NFATC1
RAP1B
RAP1A
PRKACB
CACN..
E2F8
H
Electroporated at HH22 (E3.5)---> Harvested at HH30 (E6.5)
Control
miR-19b
GFP
E2f8
SVZ
VZ
% GFP/E2f8 signal area over total area
***
ns
Control
miR-19b
I
Electroporated at HH22 (E3.5)---> Harvested at HH25 (E4.5)
Control
Sponge-19b
GFP
E2f8
% GFP/E2f8 signal area over total area
ns
***
Control
Sponge-19b
J
Electroporated at HH22 (E3.5)---> Harvested at HH34 (E8.0)
Control
miR-19b
GFP Neurod1
% GFP+; Neurod1+cells/ Total GFP+ cells
**
Control
miR-19b
K
Electroporated at HH22 (E3.5)---> Harvested at HH34 (E8.0)
Control
Sponge-19b
GFP Neurod1
% GFP+; Neurod1+cells/ Total GFP+ cells
ns
Control
Sponge-19b

Figure 1. A transient, laminar structure in the embryonic chick pallium and miR-19b mediated regulation of E2f8 and Neurod1 in in vivo condition. (A) & (B) Expression pattern of Fezf2 (ISH) and Mef2c (IHC) at E5.5 and E7.5 in chicken forebrain. 1(A) Inset shows cells double-positive for Fezf2 and Neurod1 (IHC) at SVZ . Intensity plot for Fezf2 and Mef2c. (C) Immunostaining for PH3 and Neurod1 with intensity plot. Circles show magnified view. (D) Images showing effect of overexpress CDKN1A and control on Fezf2 and Neurod1 expression. Circles showing magnified view. Bar graph showing quantification. (E) Neurod1 expression at SVZ and miR-19b (ISH) at VZ. Insets show magnified images. (F) Venn diagram displaying miRNA targets predicted by miRDB and Targetscan. Gene ontology analysis for common targets. (G) List of functionally validated targets. Red square adjacent to a gene indicates its previously reported role in process/pathway mentioned on the top row. Effect of miR-19b manipulation on E2f8 (ISH) expression (H) & (I) and on Neurod1 expression (J) & (K). Bar graph represents Mean: SE, ns= not Significant; VZ= ventricular zone, SVZ= sub-ventricular zone, DP= dorsal pallium, V= ventricle

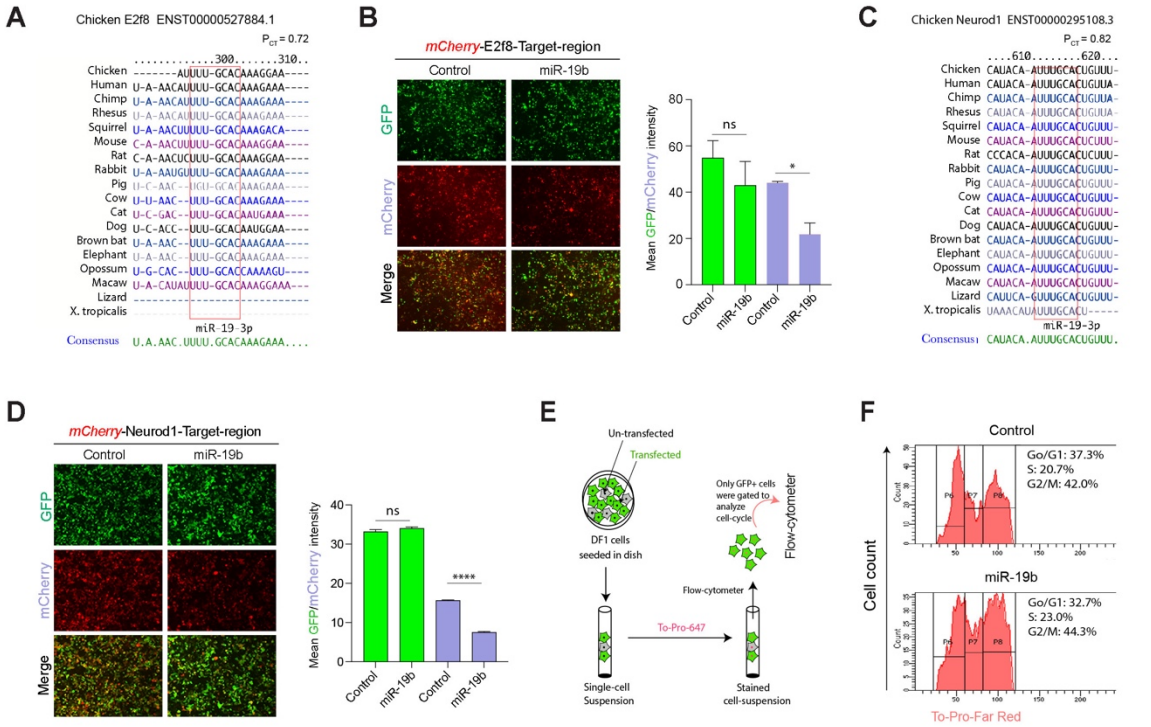
A
Chicken E2f8 ENST00000527884.1
B
mCherry-E2f8-Target-region
Control
miR-19b
GFP
mCherry
Merge
Mean GFP/mCherry intensity
ns
*
C
Chicken Neurod1 ENST00000295108.3
D
mCherry-Neurod1-Target-region
****
E
Un-transfected
Transfected
DF1 cells seeded in dish
Single-cell Suspension
To-Pro-647
Stained cell-suspension
Flow-cytometer
Only GFP+ cells were gated to analyze cell-cycle
F
Control
Go/G1: 37.3%
S: 20.7%
G2/M: 42.0%
miR-19b
Go/G1: 32.7%
S: 23.0%
G2/M: 44.3%
Cell count
To-Pro-Far Red

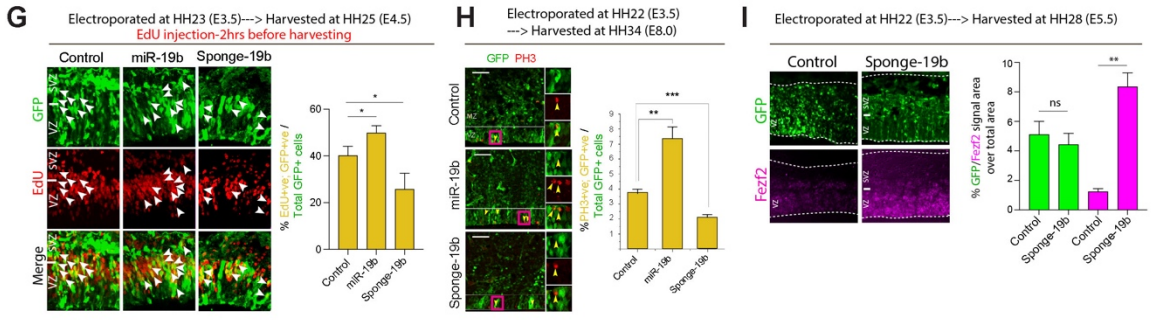
G
Electroporated at HH23 (E3.5)---> Harvested at HH25 (E4.5)
EdU injection-2hrs before harvesting
Control
miR-19b
Sponge-19b
GFP
EdU
Merge
VZ
SVZ
% EdU+ve; GFP+ve / Total GFP+ cells
H
Electroporated at HH22 (E3.5) ---> Harvested at HH34 (E8.0)
GFP PH3
% PH3+ve; GFP+ve / Total GFP+ cells
I
Electroporated at HH22 (E3.5)---> Harvested at HH28 (E5.5)
Fezf2
% GFP/Fezf2 signal area over total area

Figure 2. miR-19b regulates E2f8 and Neurod1 target regions and controls proliferation and Fezf2 expression. (A) & (C) E2f8 (ISH) and Neurod1 (IHC) target sequence with consensus miR-19b binding sites as predicted by Target scan. (B) & (D) Sensor assay to show regulation of miR-19b on target region of E2f8 and Neurod1. mCherry intensity was quantified and plotted. Data represent mean ± s.e.m., n=4 wells, t-test was performed, **$p \leq 0.01$ and ****$p \leq 0.0001$. . (E) Schema for flow cytometry experiment. (F) Cell cycle distribution of DF1 cells transfected with control, miR-19b expressing constructs. (G) & (H) Cell proliferation analysis by EdU-labeling & PH3 (IHC) upon miR-19b manipulation. White/Yellow arrowheads indicate double-positive cells . (quantification and statistical analysis to be added) (I) Effect of miR-19b inhibition on Fezf2 expression. Bar graph plotted for quantification. Bar represents : Mean ± S.E.M.